RADIATIVE TRANSFER IN CIRCUMSTELLAR DUST CLOUDS

A. D. CODE

Washburn Observatory, University of Wisconsin, Wis., U.S.A.

Abstract. Radiative transfer methods are used to show how and to what extent the usual techniques relating color excess to optical depth through circumstellar material are not applicable.

1. Introduction

The manner in which the observed flux from a star is modified by interstellar grains depends upon the spatial distribution as well as the optical properties of the grains. It is the purpose of this paper to describe the radiation transfer for several simple models in which the distinction between interstellar extinction and interstellar absorption becomes important.

If the interstellar grains are distributed along the path between the source and the observer in such a way that only an infinitesimal fraction of the scattered radiation appears in the field of view, the stellar flux is simply reduced by the extinction optical depth exponentially. The derivation of interstellar extinction curves determined by taking the ratio of a reddened and an unreddened star assumes this to be the case. If, however, scattering is produced by a nearby cloud, the extinction curve can be significantly modified. Collins and Code (1965) discussed this case for isotropic conservative scattering and Capriotti (1967) applied these considerations to the Balmer decrement in diffuse nebulae. In a series of papers by Mathis (1970, 1971, 1972) the problem of internal dust in gaseous nebulae has been investigated by an iterative numerical technique for a variety of geometries and albedos. More recently the wavelength dependence of interstellar extinction has been extended into the infrared (Johnson, 1968) and the vacuum ultraviolet (Stecher, 1959; Bless and Savage, 1972). In these spectral regions the extinction is highly non-linear and therefore provides important information on the nature of the interstellar grains. In these investigations significant variations in the derived extinction curves were found from star to star and region to region. Hallam (1959) was the first to show that variations in the law of reddening were correlated with the presence of surrounding diffuse nebulae. The most anomalous case so far documented is for the Trapezium, θ Orionis (c.f. Carruthers, 1969). It is important to separate the variations in extinction caused by differences in the nature of the interstellar grains from those produced by multiple sacttering in a nearby cloud. In their classical discussion of diffuse galactic light, Henyey and Greenstein (1941) emphasized the fact that multiple scattering rather than the precise geometry was the dominant feature in determining the modification of the stellar radiation produced by interstellar grains.

A discussion of radiative transfer in an interstellar or circumstellar dust cloud re-

Greenberg and Van de Hulst (eds.), Interstellar Dust and Related Topics, 505–515.
All Rights Reserved. Copyright © 1973 by the IAU.

https://doi.org/10.1017/S007418090005467X Published online by Cambridge University Press

quires knowledge of both the extinction cross-section and the albedo of the grains. To appreciate the importance of these considerations for a circumstellar dust cloud one need only consider the dramatic difference between the two limiting cases. If the surrounding dust cloud were spherically symmetric then in the case of pure scattering, where the albedo is unity, all the stellar radiation would escape and the luminosity and spectral distribution of the star would be unchanged. Unless we could resolve the circumstellar shell we would not know it was there. On the other hand, if the grains were pure absorbers, namely an albedo of zero, the radiation at a particular wavelength would be reduced by $e^{-\tau_\lambda}$. The total luminosity would remain the same; however, the absorbed radiation would reappear as thermal radiation in the infrared provided all energy transport is radiative.

The general characteristics of the interstellar extinction curve consist of a toe in the infrared, a nearly linear increase from 8000 Å to 4000 Å, a shoulder between 4000 Å and 3000 Å, a strong peak around 2200 Å followed by a minimum near 1600 Å, and a rise to shorter wavelengths. The albedo of the interstellar grains is uncertain. Code (1971) has discussed evidence for a high albedo shortward of the 2200 Å bump. Witt and Lillie (1972) have derived an albedo curve in the spectral region from 4250 Å to 1400 Å from measures of the diffuse galactic light utilizing OAO-2 data. The outstanding feature of their results is a pronounced decrease in albedo around 2200 Å, which is coincident with the extinction curve bump, followed by a rapid rise in albedo shortward of 2000 Å. This is a difficult observational problem and the detailed albedo curve is probably quite uncertain although the decrease in albedo near 2200 Å is consistent with the data. A significant decrease in albedo at 2200 Å is also consistent with the identification of this feature with the presence of graphite particles by Stecher (1969), Bless and Savage (1972), Gilra (1971), and Wickramasinghe and Nandy (1971). Gilra (1972) has argued on rather general grounds that whatever constituent is responsible for the bump, the feature is due to an absorption process. We shall assume this to be true and examine the consequences.

In the discussion to follow we shall assume that the extinction curve is the Johnson (1968) Cygnus curve joined to the Bless-Savage (1972) 'average' ultraviolet curve and that the albedo is represented by the Witt-Lillie (1972) results in the ultraviolet and is of the order of 0.6 in the visual (Van de Hulst and de Jong, 1969). Figure 1 shows the adopted extinction curve for a $B-V$ color excess of 1 mag. and the assumed variation of albedo that shall be adopted for illustrative purposes. It is the purpose of this paper to indicate the effect such particles would have on the observed stellar flux for several simple models.

2. Plane Parallel Slab

We consider first a star illuminating a plane parallel slab of total optical thickness, τ_λ, and albedo $\tilde{\omega}$. The total energy reflected plus the direct stellar radiation in the direction (μ, φ) follows from the physical interpretation of the X-function (Van de Hulst, 1948; Chandrasekhar, 1950) and is in fact just $X(\mu)$ times the stellar flux in the direction

https://doi.org/10.1017/S007418090005467X Published online by Cambridge University Press

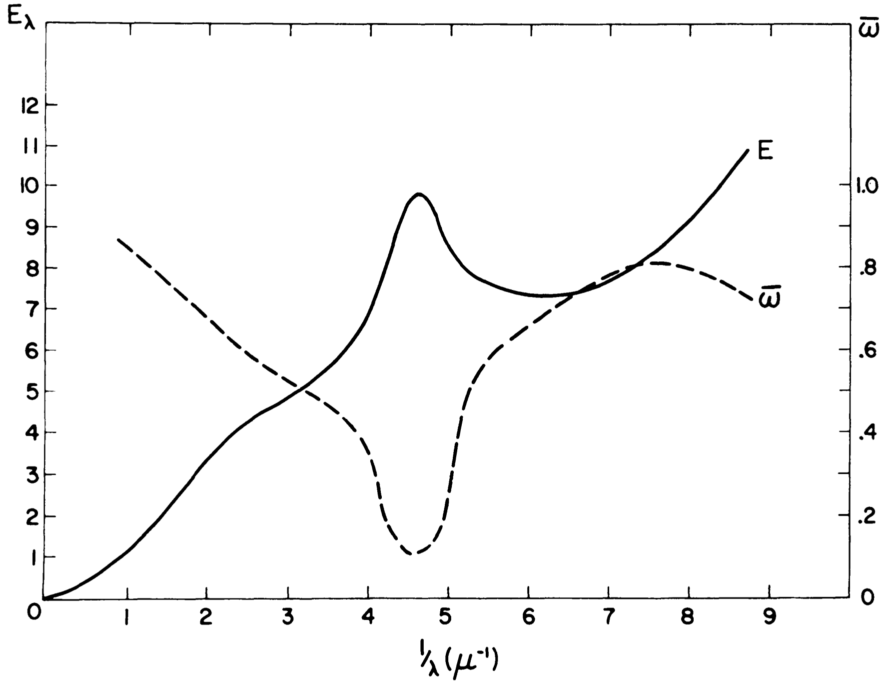

Fig. 1. The adopted extinction and albedo curves. The solid line shows the extinction in magnitude for a $B-V$ color excess of 1 mag. plotted against wavenumber in μ^{-1}. The dashed curve represents the assumed variation of albedo as a function of wavenumber as given by the right hand coordinate.

$I(\mu, \varphi)$. Similarly the total diffusely transmitted energy plus the direct transmitted energy in the direction (μ, φ) is proportional to $Y(\mu)$. Thus

$$\begin{aligned} E(\varphi, \phi)_R &= X(\mu)F^*(\mu, \varphi) \\ E(\mu, \varphi)_T &= Y(\mu)F^*(\mu, \varphi), \end{aligned} \tag{1}$$

where $F^*(\mu, \varphi)$ is the stellar flux that would be observed in the direction (μ, φ) if the plane plarallel slab were not there. If the field of view is restricted so that less and less of the surface of the slab is seen, the transmitted radiation approaches just that of the direct transmitted radiation $F^*e^{-\tau/\mu}$. One can expect cases, however, where most of the diffusely reflected or transmitted radiation will be observed. For example, virtually all the reflected energy, in the direction (μ, φ) would be observed in a field of view of 1′ for a star located 100 astronomical units in front of the slab if its distance were the order of 1 kpc.

In the case where the star is observed through the slab, two qualitative features are clear. Due to the addition of the diffusely transmitted light the extinction derived by the usual techniques would be very much smaller than if only the direct transmitted radiation is observed. Secondly, any absorption feature would be enhanced since for low albedos the diffuse radiation is small. The extinction curve resulting from the transmission of light through a slab with a visual optical depth of unity, for example, would

https://doi.org/10.1017/S007418090005467X Published online by Cambridge University Press

show a strong enhancement of the 2200 Å absorption bump if the optical properties were similar to Figure 1. The results do not differ greatly from those found for the circumstellar shells discussed in the next section; see, for example, Figure 4. For the reflection case the diffuse reflection field behaves in the same manner; however, to this radiation must be added the direct starlight and the total luminosity in the hemisphere on the reflecting side of the slab would vary from the stellar luminosity to twice this value. Although the star would appear brighter at all wavelengths than in the absence of the reflecting slab, it would appear reddened in the optical region for particles with the optical properties exhibited by Figure 1. The maximum extinction inferred by standard techniques should not exceed 0.75 mag. The increased brightness would affect the derived distance modulus.

3. Circumstellar Envelopes

We now consider the case of a spherically symmetric dust envelope surrounding a star. Huang (1969, 1971) has considered the radiative transfer in dust shells in the framework of the Eddington approximation for both thick and thin shells. His study was concerned with the transfer of stellar radiation into the infrared and he divided the radiation field into two spectral regions in which the albedo was taken to be constant. His results, therefore, give only the gross spectral distribution of the emergent flux. Furthermore, the variation of albedo with wavelength is an important feature of the problem. Huang's technique has been extended by Apruzese (1972) to consider three or more spectral regions, which then makes it possible to determine the spectral distribution by shifting the third wavelength band across the spectrum. Some of Apruzese's results will be noted later. Mathis (1972) has also carried out numerical integrations for a few cases of spherical dust envelopes for the stellar case to which we shall refer.

Let us first consider the radiation transfer problem in a spherical shell in the simplest approximation which still preserves the basic features of the problem, namely multiple non-conservative scattering. If κ represents the mass absorption coefficient and σ the mass scattering coefficient, then the extinction optical depth is given by

$$\mathrm{d}\tau = -(\kappa+\sigma)\varrho\,\mathrm{d}x \tag{2}$$

and the albedo by

$$\varpi = \frac{\sigma}{\kappa+\sigma}. \tag{3}$$

We shall simply divide the radiation into a forward and a backward stream (Schwarzschild approximation). In this case the equation of radiative transfer becomes simply

$$\frac{\mathrm{d}I_+}{\mathrm{d}\tau} = I_+ - \frac{\varpi(1+g)}{2}I_+ - \frac{\varpi(1-g)}{2}I_- \tag{4}$$

$$-\frac{\mathrm{d}I_-}{\mathrm{d}\tau} = I_- - \frac{\varpi(1-g)}{2}I_+ - \frac{\varpi(1+g)}{2}I_-, \tag{5}$$

https://doi.org/10.1017/S007418090005467X Published online by Cambridge University Press

where g is the Henyey-Greenstein phase function, which in this approximation is

$$g = \frac{\sigma_+ - \sigma_-}{\sigma}, \tag{6}$$

where σ_+, σ_- are the scattering cross-sections in the forward and backward direction, and σ their sum. The appropriate boundary conditions for a spherical shell are that there be no incident radiation on the outside boundary where $\tau = 0$. That is

$$I_-(0) = 0. \tag{7}$$

If the radius of the inner surface of the envelope is large with respect to the stellar radius, then the radiation incident on the inner boundary is equal to the stellar intensity, I^*, plus the radiation scattered from the inner boundary. Thus at $\tau = \tau_1$

$$I_+(\tau_1) = I_* + I_-(\tau_1). \tag{8}$$

The solution of Equations (4) and (5) under the boundary conditions (7) and (8) is straightforward. The ratio of the emergent luminosity to that of the stellar luminosity is

$$\frac{L}{L_*} = \frac{I_+(0)}{I_*} = \frac{2}{(1+\zeta)e^{\xi\tau_1} + (1-\zeta)e^{-\xi\tau_1}}, \tag{9}$$

where

$$\zeta = \sqrt{(1-\varpi)/(1-\varpi g)} \tag{10}$$

and

$$\xi = \sqrt{(1-\varpi)(1-\varpi g)}. \tag{11}$$

For isotropic scattering $g = 0$ and for a completely forward scattering phase function $g = 1$. In the limit $g = 1$ the solution is exact, since with spherical symmetry there would be only a radial stream of radiation. For $g = 0$ the approximation is still very good, differing from numerical calculations by less than 10% in most cases. The dash-dot curve in Figure 2 shows a plot of L/L^* as a function of extinction optical depth and albedo determined from Equation (9) for isotropic scattering. Numerical results obtained by Mathis (1972) and Apruzese (1972) are indicated by the open circles and open triangles respectively. For an albedo of one, all the radiation escapes and $L/L^* = 1$. For an albedo of zero, we have the case of pure absorption and Equation (9) becomes simply $e^{-\tau}$, shown by the lower envelope. Even for albedos very near to unity the multiple scattering at high optical depths increases the effective absorption optical depth. In the two stream approximation given by Equation (9) the ratio of the inner radius to the outer radius does not enter, as is clear from the geometry of the two stream approximation. Mathis' results are for a ratio of radii of 0.2 and he finds essentially the same value for any smaller ratio.

A somewhat closer approximation is obtained by noting that in the exact solutions for a plane parallel atmosphere the ratio of transmitted intensities for two different

https://doi.org/10.1017/S007418090005467X Published online by Cambridge University Press

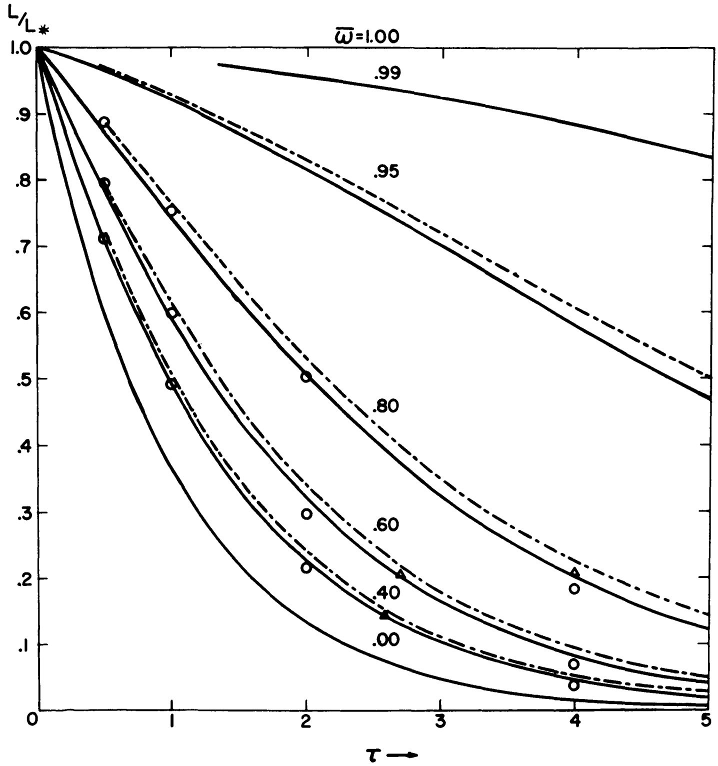

Fig. 2. The ratio of emergent luminosity to the stellar luminosity as a function of extinction optical depth and albedo for $g = 0$. The solid lines give the results obtained from Equation (12), while the dash-dot lines are for the two stream approximation given by Equation (9). Each set of curves is labeled by its appropriate albedo, $\bar{\omega}$. The open circles are from the results by Mathis (1972) for a ratio of radii of 0.2. The open triangles are from calculations by Apruzese (1972) for a ratio of radii of 0.001. Mathis quotes accuracies better than 1% for $\tau < 1$, 3% for $\tau = 2$, and 10% for $\tau = 4$.

albedos is not very sensitive to the angle of incidence. The equation

$$\frac{L}{L_*} = e^{-\tau} + (1 - e^{-\tau}) \frac{J(\bar{\omega})}{J(1)}, \tag{12}$$

where

$$\frac{J(\bar{\omega})}{J(1)} = \frac{Y(\bar{\omega}, 1) - e^{-\tau_1}}{Y(1, 1) - e^{-\tau_1}} \tag{13}$$

is in excellent agreement with detailed numerical calculations. Here $Y(\bar{\omega}, 1)$ refers to the Y-function for an albedo $\bar{\omega}$, at normal incidence, $\mu = 1$. The result of applying Equation (12) is shown as the solid curve in Figure 2.

If the ratio of radii is near unity the ratio of luminosities is given by the thin shell case which is the same as a plane parallel atmosphere with the appropriate boundary condition. This can be solved exactly by iteration using the X, Y functions and is

https://doi.org/10.1017/S007418090005467X Published online by Cambridge University Press

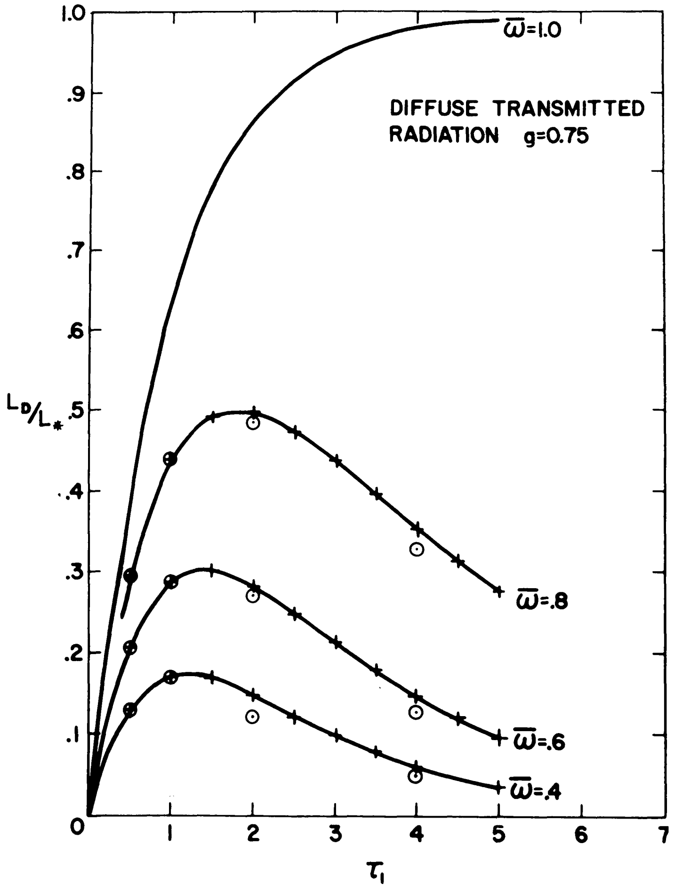

Fig. 3. Diffuse transmitted luminosity for $g = 0.75$. The solid lines are from Equation (9) where the direct transmitted component, $e^{-\tau}$, has been subtracted. The open circles are from the numerical calculations by Mathis (1972). The albedo for each curve is indicated.

approximately

$$\frac{L}{L_*} = \frac{F^\circ_{\text{trans}}/F_*}{1 - F^\circ_{\text{ref}}/F_*}, \tag{14}$$

where F°_{trans} and F°_{ref} are the total transmitted and reflected fluxes for a plane parallel atmosphere with normal incident flux. The ratios of luminosities given by Equation (14) are less than those found for the case of large curvature (small ratios of inner to outer radius). This is because large angle scattering traverses a larger optical depth in a plane parallel atmosphere than in a curved atmosphere. The luminosity curve given by (14) has the same shape and qualitatively the results insofar as they affect the extinction curve are the same. Figure 3 shows a comparison of the results obtained for $g = 0.75$ from Equation (9) with the calculations by Mathis. The agreement is excellent. The quantity plotted in Figure 3 is the ratio of the diffuse transmitted luminosity

https://doi.org/10.1017/S007418090005467X Published online by Cambridge University Press

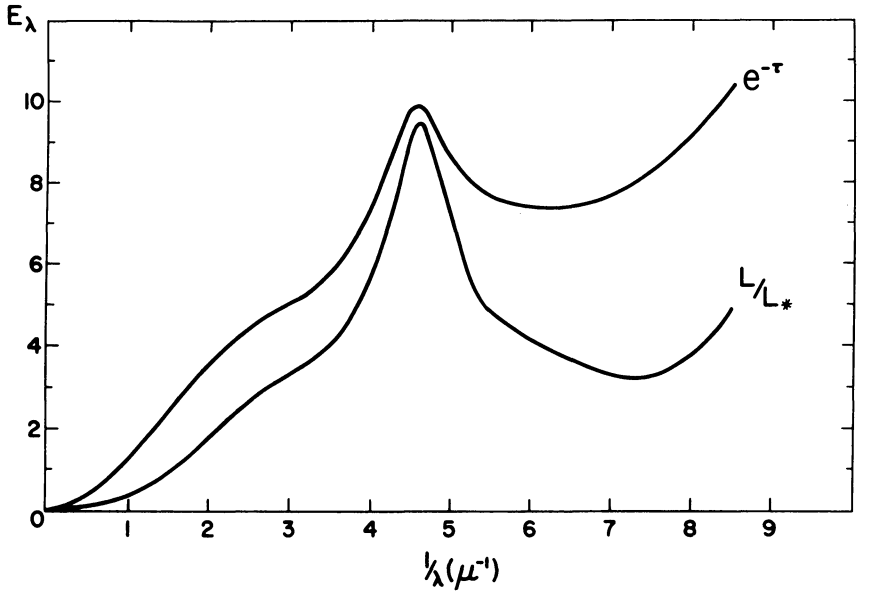

Fig. 4. Extinction by a circumstellar dust cloud. The light solid line is the same as the extinction curve shown in Figure 1. The heavy solid line shows the extinction curve that would be derived if the luminosity were modified according to Equation (9) for a circumstellar envelope.

to the stellar luminosity to illustrate the character of this field. The total luminosity is obtained by adding the direct transmitted radiation, $e^{-\tau}$, to the diffuse field.

For the purpose of determining the effect of a circumstellar dust cloud on the derived extinction curve, it is sufficient to employ the simple expression given by Equation (9). Figure 4 compares the standard extinction curve for a visual absorption of 3 mag. ($E_{B-V} = 1.0$) with the extinction curve found for a circumstellar shell of the same optical depth if the albedo varies as in Figure 1. Note the enhanced 2200 Å peak and the low apparent extinction in the 1500 Å region.

It is appropriate at this point to comment on the anomalous extinction curve found for θ Orionis (Carruthers, 1969; Bless and Savage, 1972). In these measurements the possibility of including significant scattered light is very real since the field of view included all the components of θ^1 and θ^2 Orionis as well as a significant part of the nebula. They found that the extinction in the 1500 Å region is about the same as in the visual. This is true of the results plotted in Figure 4. The bump at 2200 Å, however, is found observationally to be very small in contrast to the enhancement shown in Figure 4. If the 2200 Å feature is due to absorption, all the transfer models considered in this paper yield an enhancement of the bump and the explanation of the anomalous reddening for θ Orionis must result from an actual difference in the nature of the grain composition or size distribution. The possibility that contributions from an atomic continuum and reflected flux, however, still deserves consideration. The Trapezium is a very complicated system.

Figure 5 shows a comparison of the color excesses obtained with the UBV system if

https://doi.org/10.1017/S007418090005467X Published online by Cambridge University Press

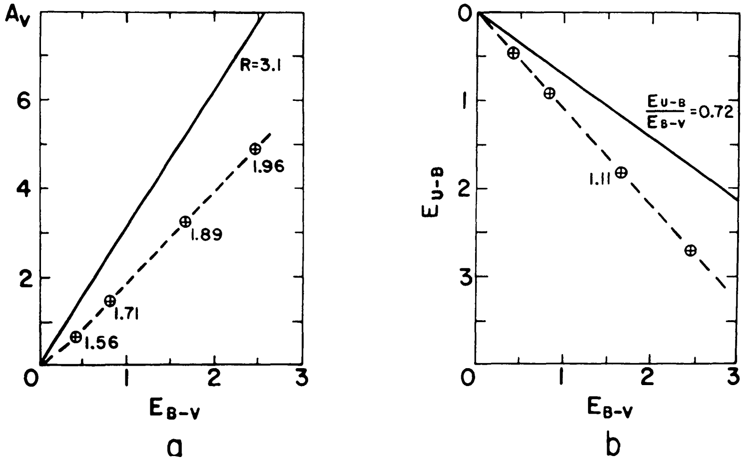

Fig. 5. (a) Total visual absorption vs $B-V$ color excess for the average extinction curve shown in Figure 1, solid curve, and for a circumstellar envelope, dashed curve. The ratio of total to selective absorption is indicated along the curve. (b) $U-B$ color excess vs $B-V$ color excess is plotted for average extinction curve and circumstellar envelope.

the extinction is circumstellar. The ratio of total to selective absorption is smaller, increasing with optical depth, and the ratio E_{U-B}/E_{B-V} is greater. The moral to be derived from these curves is obvious. Inferences as to the total optical depth from color measurements should be accepted only with reservation if there is reason to suspect that the dust is near the star.

4. Discussion

The presence of a circumstellar shell may modify the observed stellar radiation in several ways. It may be that a part of the radiant energy is converted into kinetic energy or into expansion of the dust cloud. In this case the total radiant energy is not conserved in passing through the dust shell. If the luminosity remains constant we can expect the radiation in the ultraviolet and visual to be redistributed in the infrared as a result of the absorption of grains and their thermal radiation. Apruzese (1972) has attempted to construct a model to describe the infrared star HD 45677. Some of the properties of this Be star are described by Swings and Allen (1971). The spectral energy distribution consists of a continuum in the visual, characteristic of a reddened B star, and a much stronger broad maximum in the 5–10 μ region. The infrared flux is about 4 times that of the visual. Apruzese finds that a middle B star in the center of a spherical dust cloud can quantitatively account for the observed energy distribution. For large curvature he finds that the observations require an optical depth in the visual of 3.97, 2.68, or 2.12 for albedos of 0.8, 0.6, and 0.4 respectively. His calculations also give the temperature distribution of the grains in the dust envelope. For a given temperature distribution it would be possible to compute the infrared emission for particles with known optical constants. Gilra and Code (1971) have suggested that circumstellar

https://doi.org/10.1017/S007418090005467X Published online by Cambridge University Press

clouds of SiC can account for the very strong violet opacity in C and C–S stars and have predicted infrared emission due to SiC between 10 μ and 13 μ. Hackwell (1972) has reported observations of this feature. Gilra (1973) has described some other emission bands that might be expected in the infrared.

Another way in which the circumstellar cloud might modify the stellar radiation is to change the temperature distribution in the stellar atmosphere. This backwarming was first invoked to explain certain features in the behavior of long period variable stars by Merrill (1940). Some insight into the effect of this backwarming can be obtained by considering a simple grey atmosphere in the Eddington approximation. In this case the mean intensity is given by

$$J = \tfrac{3}{4}F(\tau + Q). \tag{15}$$

We then replace the boundary condition that no radiation is incident at $\tau = 0$ by the condition that a fraction α of the outward intensity is returned to the stellar surface. That is, at $\tau = 0$,

$$I_+ = I_0 \tag{16}$$

and

$$I_- = \alpha I_0 ; \tag{17}$$

then

$$J(0) = \tfrac{1}{2}I_0(1+\alpha) \tag{18}$$

and

$$F(0) = I_0(1-\alpha). \tag{19}$$

Solving (15) for Q we find that

$$J = \tfrac{3}{4}F\left(\tau + \frac{2}{3}\frac{(1+\alpha)}{(1-\alpha)}\right) \tag{20}$$

or the temperature distribution is

$$T^4 = \tfrac{3}{4}T_e^4\left(\tau + \frac{2}{3}\frac{(1+\alpha)}{(1-\alpha)}\right). \tag{21}$$

The temperature at small optical depths is increased by the radiation scattered or reemitted from the shell towards the stellar surface. For example, the temperature at an optical depth of unity is increased by about 15% if $\alpha = 0.5$. Buerger (1972) has recently computed a series of model atmospheres in which incident radiation is included. He finds effects of the same order as given by the simple grey atmosphere. It would be worthwhile carrying out more detailed calculations to determine the spectral distribution and the strength of particular atomic lines to see if the change in the stellar spectrum produced by circumstellar backwarming should be observable.

In summary, we have tried to indicate the manner in which the presence of nearby

https://doi.org/10.1017/S007418090005467X Published online by Cambridge University Press

dust clouds can influence the observed flux from stars. The discussion indicates that for stars with significant infrared excesses neither the nature of the embedded star nor the optical depth of the dust cloud can be determined by the usual techniques employing color excesses and ratios of total to selective absorption. The errors can be large. Finally, it should be remarked that features considered in this paper are also applicable to stellar systems such as galaxies (Code *et al.*, 1972).

References

Apruzese, J.: 1972, private communication.
Bless, R. C. and Savage, B. D.: 1972, *Astrophys. J.* **171**, 293.
Buerger, P. F.: 1972, *Astrophys. J.* **177**, 567.
Capriotti, E. R.: 1967, *Astrophys. J.* **148**, 318.
Carruthers, G. R.: 1969, *Astrophys. J. Letters* **157**, L113.
Chandrasekhar, S.: 1950, in *Radiative Transfer*, Oxford Press, p. 211.
Code, A. D.: 1971, in B. T. Lynds (ed.), *Dark Nebulae, Globules and Protostars*, University of Arizona Press, Tucson, p. 101.
Code, A. D., Welch, G. A., and Page, T. L.: 1972, in A. D. Code (ed.), *The Scientific Results from the Orbiting Astronomical Observatory*, NASA SP-310, p. 559.
Collins, G. W., II and Code, A. D.: 1965, *Astrophys. J.* **142**, 1576.
Gilra, D. P.: 1971, *Nature* **229**, 237.
Gilra, D. P.: 1972, in A. D. Code (ed.), *The Scientific Results from the Orbiting Astronomical Observatory*, NASA SP-310, p. 295.
Gilra, D. P.: 1973, this volume, p. 517.
Gilra, D. P. and Code, A. D.: 1971, *Bull. Am. Astron. Soc.* **3**, 379.
Hackwell, J. A.: 1972, preprint.
Hallam, K. L.: 1959, Thesis, University of Wisconsin.
Henyey, L. G. and Greenstein, J. L.: 1941, *Astrophys. J.* **93**, 70.
Huang, Su-Shu: 1969, *Astrophys. J.* **157**, 843.
Huang, Su-Shu: 1971, *Astrophys. J.* **164**, 91.
Johnson, H. L.: 1968, in B. M. Middlehurst and L. H. Aller (eds.), *Nebulae and Interstellar Matter*, University of Chicago Press, Chicago, p. 167.
Mathis, J. S.: 1970, *Astrophys. J.* **159**, 263.
Mathis, J. S.: 1971, *Astrophys. J.* **167**, 261.
Mathis, J. S.: 1972, *Astrophys. J.* **176**, 651.
Merrill, P. W.: 1940, *Spectra of Long-Period Variable Stars*, University of Chicago Press, Chicago.
Stecher, T. P.: 1969, *Astrophys. J. Letters* **157**, L125.
Swings, J. P. and Allen, D. A.: 1971, *Astrophys. J. Letters* **167**, L41.
Van de Hulst, H. C.: 1948, *Astrophys. J.* **107**, 220.
Van de Hulst, H. C. and de Jong, T.: 1969, *Physica* **41**, 151.
Wickramasinghe, N. C. and Nandy, K.: 1971, *Nature* **229**, 81.
Witt, A. N. and Lillie, C. F.: 1972, in A. D. Code (ed.), *The Scientific Results from the Orbiting Astronomical Observatory*, NASA SP-310, p. 199.

https://doi.org/10.1017/S007418090005467X Published online by Cambridge University Press